

MATHEMATICAL PRINCIPLE AND NUMERICAL RECONSTRUCTION IN REAL SPACE MEASUREMENT WITH A ROTATING BPM*

Peiyong Jiang[†], Yuan He, Zhijun Wang

Institute of Modern Physics, Chinese Academy of Sciences, Lanzhou, China

Abstract

It is difficult to measure beam profiles and monitor the beam during beam supply for high intensity high power accelerators. Based on the button pick-ups, the mathematical principle of a rotating BPM is proposed. SVD method is used to reconstruct the beam in x-y real space, and the basic parameters used in beam reconstruction are argued. The beam distribution in x-y real space is reconstructed well and compared to the reference beam. The beam reconstruction is sensitive to the electrode radius. The meshing and the grid numbers in the solution window have an import effect on the beam reconstruction.

INTRODUCTION

It is difficult to measure beam profiles for high intensity high power accelerators. The wire scanner system is often used to measure beam profiles [1]. However, the stable operation of wire scanners has much to do with beam power [2]. The beam current has to decrease below a power limit in CIADS project to protect the wire scanners, bringing the difference in x-y real space between the low intensity and the high intensity beams. Besides, the slit and Faraday cup are used to measure beam profiles.

The two methods are invasive diagnostics, which cannot be applied to the high power accelerators with the high requirement of continuity in operation such as CIADS project [3]. Meanwhile, owing to the high requirement of stability and security of CIADS, it is necessary to monitor the beam including the beam profiles dynamically and to adjust the machine parameters properly. Thus, there is a strong need to use a non-invasive beam diagnostic component to measure beam profiles during beam supply, based on which a rotating BPM is proposed mathematically.

BPM PRINCIPLE

BPM is widely used in accelerators to measure the beam orbit, beam phase and beam emittance [4,5,6]. Button pick-ups, shoe box pick-ups and stripline pick-up are the three common kinds of BPM [7]. Figure 1 shows the theory of button pick-ups. There are 4 electrodes in the top, bottom, left and right of the pipe respectively. The electrodes induct the current while a charged beam line pass through the pipe. Considering a beam with current $I(r, \phi)$ in a straight wire of infinite length in a polar coordinate system, the current density $j(a, \theta, r, \phi)$ on the pipe boundary induced by the straight wire current and its mirror current is

$$j(a, \theta, r, \phi) = \frac{I(r, \phi)}{2\pi a} \frac{a^2 - r^2}{a^2 + r^2 - 2\cos(\phi - \theta)} \quad (1)$$

where (a, θ) is an arbitrary point on the pipe boundary in a polar coordinate system, while a is the pipe radius and θ is the angle pointed to the point. (r, ϕ) is an arbitrary point in the pipe while r is the distance between the beam and the pipe center, and ϕ is the angle pointed to the beam.

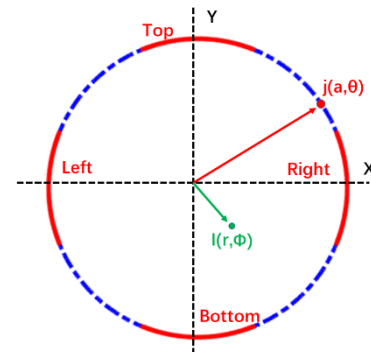


Figure 1: The theory of button pick-ups. The blue dashed circle is the pipe boundary. The red curves at top, bottom, left and right are the BPM electrodes respectively. $I(r, \phi)$ is the current of a straight wire of infinite length, and $j(a, \theta, r, \phi)$ is the induced current at the point (a, θ) in a polar coordinate system.

As for a beam with a cross section, the total induced current J on the electrode with a flare angle β is an integral as follows:

$$J(a) = \int_{-\beta/2}^{\beta/2} \int \int j(a, \theta, r, \phi) dr d\phi d\theta \quad (2)$$

The integral J changes to be a product while beta is small:

$$J(a) = \beta \int j(a, \theta, r, \phi) dr d\phi \quad (3)$$

and the average induced current B is written as:

$$B(a) = \frac{1}{\beta} = \int \int j(a, \theta, r, \phi) dr d\phi \quad (4)$$

By substituting Eq.(1) into Eq.(4), the discrete form of Eq.(4) is obtained:

$$B = M \cdot I \quad (5)$$

Where I and B are column vectors, and the lengths of I and B are corresponding to the number of straight wires of beam current and the number of BPM electrodes respectively. M is a matrix with

$$M_{b,i} = \frac{1}{2\pi a_b} \frac{a_b^2 - r_i^2}{a_b^2 + r_i^2 - 2\cos(\phi_i - \theta_b)} \quad (6)$$

where b is the b^{th} electrode, and the i is the i^{th} straight wire of beam current.

RECONSTRUCTION

Mathematically, the reconstruction is to solve Eq.(5). However, the matrix is unknown in this equation. Thus during the solving, a solution window has to be assumed,

Beam dynamics, extreme beams, sources and beam related technologies

Beam Dynamics, beam simulations, beam transport

and it changes during iteration. Figure 2 illustrates the solution window in a rotating BPM.

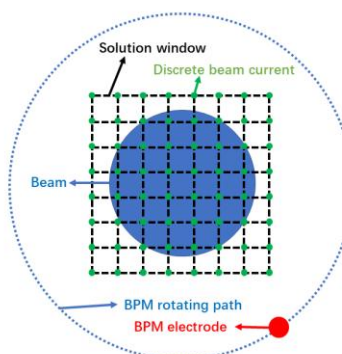


Figure 2: The solution window in a rotating BPM. The red point is the BPM electrode, and the blue dashed circle is the BPM rotating path. The blue disk is the beam which could be solved by being allocated to the green points. The black dashed mesh grids are the solution window, and the green points on the mesh grids are the discrete beam current.

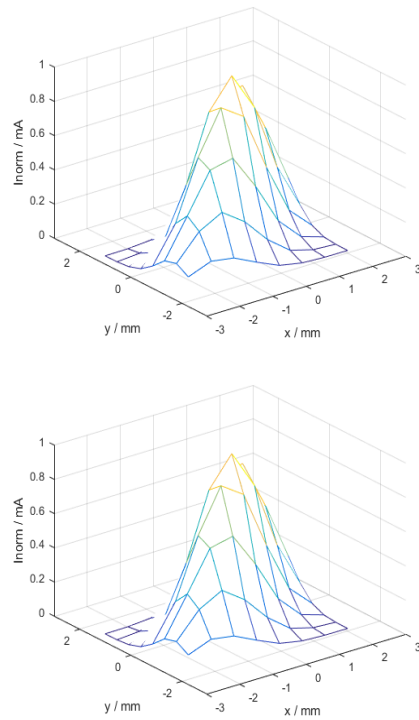


Figure 3: (a): Comparison between the reference beam distribution and the reconstruction beam distribution in X-Y real space. (a): Reference beam; (b): Reconstruction beam.

Given a solution window, M is known, and then the beam distribution on the window grids is solved. If the solved beam is in the solution window, the process finishes; Otherwise the solution window is reset and enters a iterative loop to update M .

The solving process of Eq. (5) is based on ‘singular value decomposition’ (SVD). The matrix M is decomposed as:

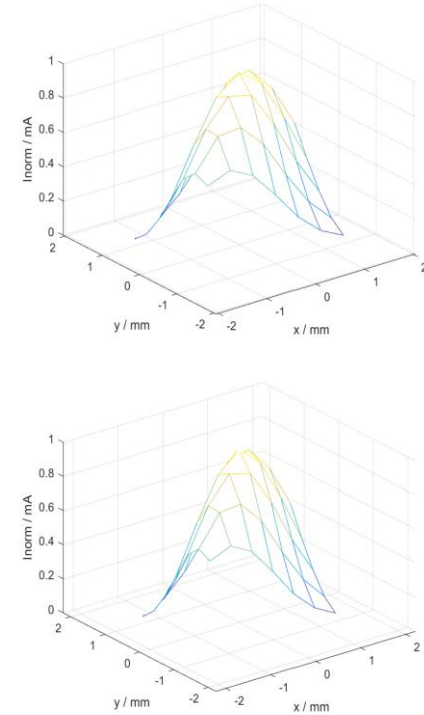
$$M = U \cdot S \cdot V^T \quad (7)$$

The beam current I on the grids is solved as:

$$I = V \cdot S^{-1} \cdot U^T \cdot B \quad (8)$$

The electrode radius has an important impact on the reconstruction. The beam expresses to be an electric monopole if the electrode radius is much larger than the beam size, and to be an electric multipole if the electrode radius is similar to the beam size. If the beam expresses as a monopole, the induced current along rotating path is smooth, and it is difficult to express the details of the beam. Figure 5 shows the reconstruction with the change of the electrode radius. The beam reconstruction makes no change while the electrode radius is restrained, and the beam reconstruction goes worse immediately if the electrode radius is up to a limit. The last plot in Figure 4 shows that the beam core which is further from the electrode goes worse firstly. Since the electrode radius plays an important role in beam reconstruction, the inner layer of BPM expresses more details than the outer layer.

The solution window is important in the reconstruction. Since the values of significance in S which corresponds to the high orders are approximate to 0, the effective rank of determinant M is smaller than the row number of the M . But it is difficult to calculate the effective rank, and to determine how smaller the value in S is that can be ignored in beam reconstruction. The grid numbers of the solution window should be smaller than the effective rank of determinant M . Figure 5 show the experiment on the beam reconstruction with increasing the grid numbers. In this case, the rotating angle is set as 1°.



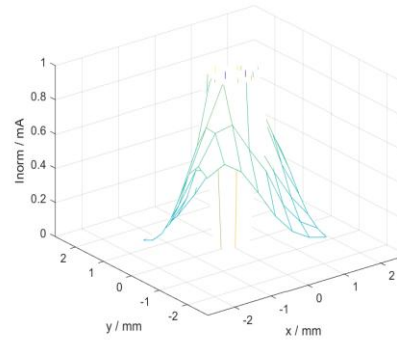
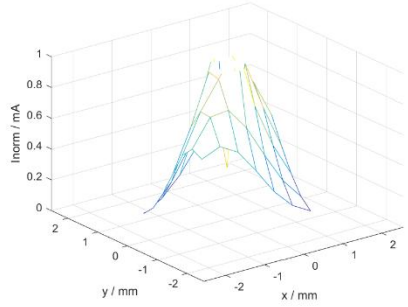
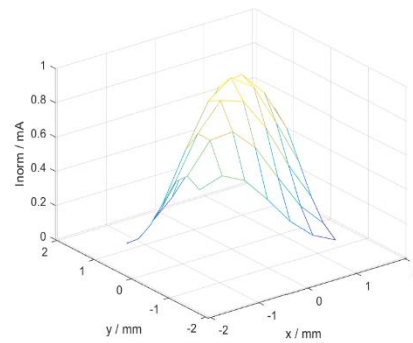
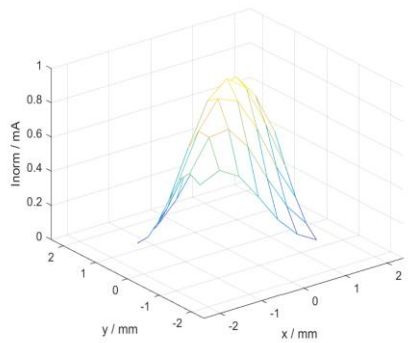


Figure 4: The comparison of the beam reconstruction in X-Y real space with the change of the electrode radius.
(a): The electrode radius is 1.2 times the size of the beam;
(b): The electrode radius is 1.3 times the size of the beam;
(c): The electrode radius is 1.4 times the size of the beam.
(d): The electrode radius is 1.5 times the size of the beam.

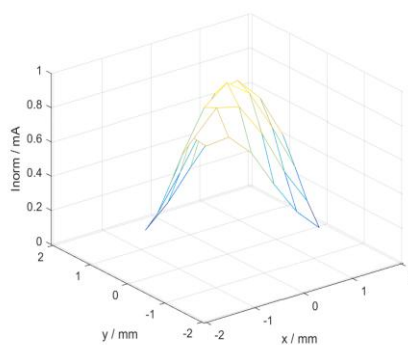
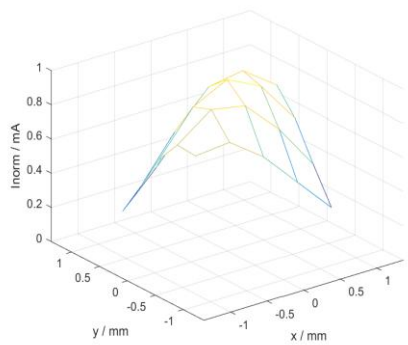


Figure 5: The comparison of the beam reconstruction in X-Y real space with the increase of grid numbers in solution window. (a): The grid numbers in solution window is (5,5);
(b): The grid numbers in solution window is (6,6); (c): The grid numbers in solution window is (7,7); (d): The grid numbers in solution window is (8,8).

CONCLUSION

A rotating BPM is proposed while the mathematic principle and numerical solution are shown and the basic parameters are argued in this paper. We hope such idea will be used in X-Y real space beam measurement as a part of conventional beam diagnostic components in high intensity high power accelerators such as CIADS.

REFERENCES

- [1] U. Hahn, N. V. Bargen, P. Castro, *et al.*, Wire scanner system for FLASH at DESY, NIMA 592 (2008) 189-196.
- [2] T. Yang, S. Fu, T. Xu, *et al.*, Thermal analysis for wire scanners in the CSNS Linac, NIMA 760(2014)10-18.
- [3] S.H. Liu, Z.J. Wang, H. Jia, *et al.*, Physics design of the CIADS 25 MeV demo facility, NIMA 843 (2017) 11-17.
- [4] M. Month. Lecture notes in physics, frontiers of particle beams: observation, diagnosis and correction. Springer Berlin, 1989, p. 46-64.
- [5] P. Strehl. Beam instrumentation and diagnostics. Springer Berlin, 2006.
- [6] A. Jansson, Non-invasive measurement of emittance and optical parameters for high-brightness hadron beams in a synchrotron, CERN/PS, 2001-014 (OP).
- [7] P. Forck, Lecture notes on beam instrumentation and diagnostics, JUAS, January-March 2011.